2018 European Control Conference (ECC)
June 12-15, 2018. Limassol, Cyprus

Distributed coordination of energy-storage capacities in virtual microgrids*

Robert W. Brehm, Hossein Ramezani and Jerome Jouffroy[1]

Abstract— **An approach for distributed coordinated scheduling of storage capacities is presented. When storage capacities are connected in the same grid, behind a common transformer substation, mutual charging and discharging can occur, which can be prevented by the herein introduced coordination method. When cooperation is incorported, storage capacities can be operated as a virtual microgrid. The cooperation between nodes is based on the formulation of a simple objective function for coordination. The cooperation objective is then combined with each node's local objective, which is the increase of self consumption, such that load is released off the the grid. A qualitative reflection on the practical use of three distributed algorithms, to solve the formulated optimisation problem is provided. The Jacobi algorithm is qualified to be preferable for large-scale networks with a great number of nodes, and the Gauss-Seidel algorithm is preferable when less nodes cooperate. To illustrate the concept and show the effect of coordination for prevention of mutual charging/discharging of storage capacities in a VMG, two comparative case-study scenario are presented.**

I. Introduction

The increasing integration of highly fluctuating, intermitent and distributed renewable energy resources has brought massive challenges to electrical grid system operation with regard to power system commitment, dispatching and reserve requirements [13]. One envisioned approach to operating this decentralised supply system is the concept of virtual microgrids (VMG) [2], [4]. A VMG bundles multiple local, installed on the same grid layer, distributed energy generation units as well as local loads and energy storage capacities, to work as a virtual sub-grid in parallel to the utility grid. VMGs are envisioned as being part of the existing distribution grid infrastructure, downstream of distribution substations and are to be implemented on top of the existing infrastructure of a supply grid, preferably in low and medium voltage grids.

In a VMG, all distributed and dispatchable supply system components have to be operated to fulfill some predefined operational objectives. This can be formulated as a mathematical optimisation problem (OP). The primary operational objective of a VMG is, to maximize the level of self-consumption, in order to release peak loads off the utility grid [10]. This is achieved by efficient dispatching of charge and discharge periods of storage capacities, such as batteries, which are co-located to renewable energy resources, for example Photovoltaic (PV) panel installations. Various battery systems, to increase the level of self-consumption in buildings, are nowadays commercially available. In research, approaches for local dispatching of a battery have been introduced based on the concept of dynamic tariffs, where the objective is economical cost reduction [5] based on price a for energy bought from the grid. The problem formulation can be focused on the perspective of residential customers [14], [6], [15] but also on the system operators perspective [7]. However, if during the dispatching process of a battery, the individual operational schedules of all batteries within a VMG are not coordinated, mutual charging and discharging of storage capacities can occur [4]. Situations occur, in which a battery is charged by discharging another battery within the same time period, and vice versa.

Coordination between nodes, to prevent mutual charging and discharging of batteries, can be managed by a central coordinator node. However, since each system node is aware of its local technical performance characteristics (constraints), the underlying physical architecture is naturally suitable for a distributed Energy Management System (EMS) for battery scheduling. The advantage of a distributed aproach is, the flexible incorporation of infrastructural and local dynamic variation of constraints (e.g. decrease of battery capacity over time and/or temperature) as well as rapid adaptation to these changes [12], [16]. Also, the distributed approach improves failure safety as well as compliance with privacy concerns, since data is not centrally aggregated. Further, no single-point of failure exists.

It was shown by [4], that mutual charging/discharging of batteries can be prevented, by a distributed algorithms which combines a consensus scheme with the Arrow-Hurwicz primal-dual algorithm. However, this approach is based on first order methods with slow convergence and per-iteration message exchange between nodes, which results in large amount of messages being exchanged between nodes.

As a contribution to the preceding work done in [4] and on battery scheduling for local buildings as introduced in [14], [6], [15], we propose a optimization problem (OP) formulation, which incorporates cooperation between the individual nodes. This prevents mutual charging and discharging of batteries so that they can be operated as a VMG. Further we introduce three algorithms to solve the given OP in a distributed architecture and qualify them with regards to practical applicability.

After this introductory section, in Section II, we present the formulation as OP which incorporates coordination between nodes to prevent mutual charging/discharging. In

*This work was supported by the European Commission through the carpeDIEM project which is funded by the INTERREG 5A Germany-Denmark program.

[1]All authors are with SDU Mechatronics, the Mads Clausen Institute, University of Southern Denmark (e-mail: brehm@mci.sdu.dk, ramezani@mci.sdu.dk, jerome@mci.sdu.dk)

Section III, three distributed algorithms are introduced and qualified. To demonstrate the introduced scheme, in Section IV, we present the results of a case-study scenario for different buildings in a VMG, where each is equipped with local PV installations with co-located battery storage capacities. The paper ends with brief concluding remarks.

II. Coordinated Scheduling of Distributed Storage Capacities

The chosen objective for the VMG operation is the minimization of power flow over a transformer substation to an overlaying grid. In Figure 1 this is indicated by the power flow arrow $\boldsymbol{\psi}$ over the substation from/to the medium-voltage grid. Each of the EMS nodes is able to control power flow vectors to either charge or discharge local storage capacities. It is assumed that each EMS node is aware of local predictive information about load and production profiles over the time horizon to be scheduled. Also, each supply component which is managed by an EMS node is connected to a common low voltage (LV) grid. Such a scheme is provided in LV residential grids as shown in Figure 1.

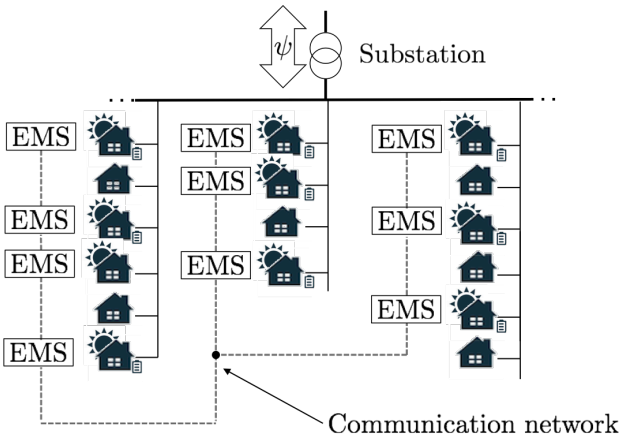

Fig. 1. Example of a distributed EMS at local low voltage grid.

A. Nodes Interconnection

For efficient operation of the distributed storage system and for prevention of mutual charging/discharging, all EMS nodes coordinate charge and discharge schedules with neighboring nodes such that a coordinated global schedule for all storage capabilities is achieved. The underlying optimization problem is structured so that for each node, there are local constraints. these are: power flow limits for charging/discharging of a battery, capacity constraints and state-of-charge levels to be maintained. Strict observance of these criteria can be maintained locally by each individual agent during the scheduling (dispatching) process. Additionally, it is stipulated that all batteries are operated synchronously. Meaning, that batteries do not compensate each other by charging a battery at one system node by discharging a battery at another node. This is maintained by adding a coordination term, to be minimised, to the local objective function.

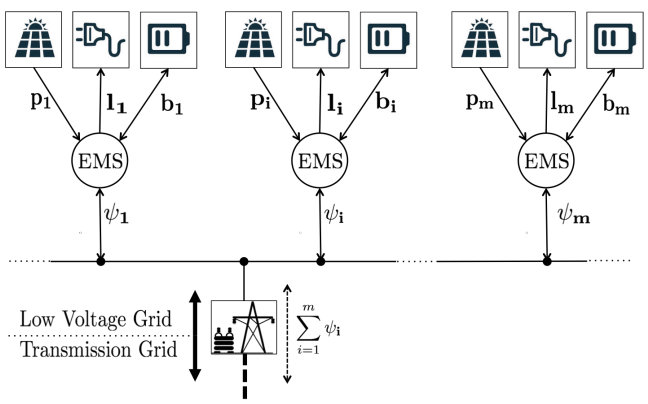

Fig. 2. Local node model, controlled by a local EMS. All nodes are connected behind a common transformer substation.

B. Local nodes model

The objective of each individual node is the reduction of energy flow from/to the grid, by efficient operation of the local storage capacity, as shown in Figure 2, such that its self-consumption is maximised. As previously suggested by [14], the chosen objective in the local model for each node, is the minimisation of energy flow from/to the overlaying grid using the minimisation of a quadratic objective function:

$$\sum_{j=1}^{s} [\psi_i^j]^2, \ \forall i \in \{1, \ldots, m\}, \tag{1}$$

where m denotes the number of distributed EMS nodes interconnected in a distributed prosumer system, s is the number of equal time intervals of length Δt spread over the scheduling time horizon T. Furthermore, ψ_i^j, $\forall j \in \{1, \ldots, s\}$, denotes the averaged power in kW supplied from, or fed to the grid by a node over a period $[t_{j-1}, t_j]$.

The given objective in (1) is subject to a number of constraints. Each node has a local energy balance constraint, which is defined as:

$$\mathbf{b}_i + \boldsymbol{\psi}_i = \mathbf{l}_i - \mathbf{p}_i, \qquad \forall i \in \{1, \ldots, m\}. \tag{2}$$

Here, $\boldsymbol{\psi}_i \in \mathbb{R}^s$ with $\boldsymbol{\psi}_i = [\psi_i^1, \ldots, \psi_i^s]^T$ and $\mathbf{b}_i \in \mathbb{R}^s$, $\mathbf{b}_i = [b_i^1, \ldots, b_i^s]^T$ denotes the averaged power flow in kW at node i into and out of its storage capacities. Note that if $b_i^j \in \mathbb{R}_{>0}$ or if $b_i^j \in \mathbb{R}_{<0}$ the battery is charging or discharging, respectively. The averaged power flow to local loads in kW at node i, is denoted by $\mathbf{l}_i \in \mathbb{R}^s_{\geq 0}$, with $\mathbf{l}_i = [l_i^1, \ldots, l_i^s]^T$. The averaged power flow in kW at node i from local generation units is denoted by $\mathbf{p}_i \in \mathbb{R}^s_{\geq 0}$, with $\mathbf{p}_i = [p_i^1, \ldots, p_i^s]^T$.

The upper and lower limits for the power flow into and out of the storage capacity are treated by maximum charging discharging constraints which are defined by the individual storage capacity in use. Thus we have

$$B_i^- \leq b_i^j \leq B_i^+, \qquad \forall j \in \{1, \ldots, s\}, \forall i \in \{1, \ldots, m\}. \tag{3}$$

where $B_i^- \in \mathbb{R}_{\leq 0}$ denotes the maximum discharge power and $B_i^+ \in \mathbb{R}_{\geq 0}$ the maximum charge power of each individual storage capacity at node i.

The state of charge of a battery is constrained by the capacity C_i of the storage capacity, such that:

$$0 \leq \boldsymbol{\xi_i} \leq C_i \begin{bmatrix} 1 \\ \mathbb{1} \end{bmatrix}, \qquad \forall i \in \{1, \ldots, m\}, \tag{4}$$

where $\mathbb{1} \in \mathbb{R}^s$ denotes an all-1 column vector of length s, and $\boldsymbol{\xi}_i = [\xi_i^0, \ldots, \xi_i^s]^T$ with $\boldsymbol{\xi}_i \in \mathbb{R}_{\geq 0}^{s+1}$ denote the state of charge at the time interval $[0, s\Delta t]$. Hence, the state of charge at any interval h is given by

$$\xi_i^h = \xi_i^0 + \sum_{j=1}^{h} b_i^h \Delta t, \qquad \forall i \in \{1, \ldots, m\}, \tag{5}$$

where ξ_i^0 denotes the initial and ξ_i^h the state of charge at interval h, respectively.

As a requirement, over the scheduling time horizon T, it is assumed that the final state of charge ξ_i^s should equal the initial state of charge, such that

$$\xi_i^s = \xi_i^0, \text{with: } 0 \leq \xi_i^0 \leq C_i, \qquad \forall i \in (1, \ldots, m), \tag{6}$$

and

$$\sum_{j=1}^{s} b_i^j = 0, \qquad \forall i \in 1, \ldots, m. \tag{7}$$

Note that this scheme can be modified in order to follow some gradients to reflect daily, weekly or seasonal variations or other parameters.

C. Coordination

The overlaying interaction topology of EMS nodes in a communication network is represented by the graph $G = (\mathcal{V}, \mathcal{E})$ with the set of EMS nodes $\mathcal{V} = \{1, \ldots, m\}$ and a set of edges $\mathcal{E}$ denoted by (i, j), with $(i, j) \in \mathcal{V}$.

In order to incorporate inter-node cooperation, under the assumption of a connected graph, the following cooperation objective function can be defined:

$$J_{co} = \frac{1}{2} \sum_{i \in \mathcal{V}} \left(\sum_{j \in \mathcal{N}_i} \mathbf{r}_i - \mathbf{r}_j \right)^2 \tag{8}$$

where $\mathcal{N}_i$ is the set of neighbouring nodes that are connected to node i, and $\mathbf{r}_i$ is the relative storage power flow profile vector for each node i. The latter is defined as

$$\mathbf{r}_i = \mathbf{C}_i^{-1} \mathbf{b}_i, \ \forall i \in \{1, \ldots, m\}. \tag{9}$$

where, $\mathbf{C}_i \in \mathbb{R}^{s \times s}$ is defined as

$$\mathbf{C}_i = \text{diag}(C_i, \ C_i, \ \cdots \ , C_i). \tag{10}$$

Equation (8) represents an appraisal for cooperation for each node and is proportional to the level of cooperation each node adopts, thus the equality of individual relative storage power flow vectors. Objective (8) can be written in matrix form as:

$$J_{co} = \frac{1}{2} \mathbf{r}^T \mathbf{L}^T \mathbf{L} \mathbf{r}, \tag{11}$$

where $\mathbf{L}$ is the graph Laplacian matrix and $\mathbf{r} = [\mathbf{r}_1, \ldots, \mathbf{r}_m]^T$. Rewriting (11) yields

$$J_{co} = \frac{1}{2} \mathbf{b}^T \boldsymbol{\Gamma} \mathbf{b}, \tag{12}$$

where $\mathbf{b} = [\mathbf{b}_1, \ldots, \mathbf{b}_m]^T$ and

$$\boldsymbol{\Gamma} = \mathbf{C}^{-1} \mathbf{L}^T \mathbf{L} \mathbf{C}^{-1}, \tag{13}$$

with:

$$\mathbf{C} = \text{diag}(\mathbf{C}_i, \ldots, \mathbf{C}_m). \tag{14}$$

D. Optimisation problem

By adding the coordination objective (12) to the introduced local objective function (1), inter-node cooperation can be incorporated as follows:

$$J = \frac{1}{2} \Big(\boldsymbol{\psi}^T \boldsymbol{\psi} + \rho \ \mathbf{b}^T \boldsymbol{\Gamma} \mathbf{b} \Big), \tag{15}$$

with $\boldsymbol{\psi} = [\boldsymbol{\psi}_1, \ldots, \boldsymbol{\psi}_m]^T$ and where ρ denotes a weighting factor as a trade-off between local objective and cooperation with the set of neighbouring nodes $\mathcal{N}_i$.

Based on the objective function (15) and the introduced constraints, the following quadratic programming problem can be defined for the VMG:

$$\begin{aligned} &\min_{\mathbf{x}} \ \tfrac{1}{2} \mathbf{x}^T \mathbf{Q} \mathbf{x} \\ &\text{s. t.} \begin{cases} \mathbf{A}\mathbf{x} = \boldsymbol{\alpha} \\ \mathbf{B}\mathbf{x} \leq \boldsymbol{\beta} \end{cases} \end{aligned} \tag{16}$$

Here, $\mathbf{x} = [\mathbf{x}_i, \ldots, \mathbf{x}_m]^T$, with $\mathbf{x_i} = [\boldsymbol{\psi_i}, \mathbf{b_i}]^T$ and $\mathbf{Q} \in \mathbb{R}_{\geq 0}^{2ms \times 2ms}$ is given by

$$\mathbf{Q} = \begin{bmatrix} \mathbf{I} & \mathbf{0} & \mathbf{0} & \mathbf{0} & \cdots & \mathbf{0} \\ \mathbf{0} & \rho\boldsymbol{\Gamma}_{11} & \mathbf{0} & \rho\boldsymbol{\Gamma}_{12} & \cdots & \rho\boldsymbol{\Gamma}_{1m} \\ \mathbf{0} & \mathbf{0} & \mathbf{I} & \mathbf{0} & \cdots & \mathbf{0} \\ \mathbf{0} & \rho\boldsymbol{\Gamma}_{21} & \mathbf{0} & \rho\boldsymbol{\Gamma}_{22} & \cdots & \rho\boldsymbol{\Gamma}_{2m} \\ \vdots & \vdots & \vdots & \vdots & \ddots & \vdots \\ \mathbf{0} & \rho\boldsymbol{\Gamma}_{m1} & \mathbf{0} & \rho\boldsymbol{\Gamma}_{m2} & \cdots & \rho\boldsymbol{\Gamma}_{mm} \end{bmatrix}, \tag{17}$$

with $\mathbf{I}$ being an $s \times s$ identity matrix and the other matrices in (16) are defined as:

$$\begin{aligned} &\mathbf{A} = \text{blkdiag}(\mathbf{A}_1, \mathbf{A}_i, \ldots, \mathbf{A}_m), \\ &\boldsymbol{\alpha} = [\boldsymbol{\alpha}_1^T \ \boldsymbol{\alpha}_i^T \ \ldots \ \boldsymbol{\alpha}_m^T]^T, \\ &\mathbf{B} = \text{blkdiag}(\mathbf{B}_1, \ \mathbf{B}_i, \ldots, \ \mathbf{B}_m), \\ &\boldsymbol{\beta} = [\boldsymbol{\beta}_1^T \ \boldsymbol{\beta}_2^T \ \ldots \ \boldsymbol{\beta}_m^T]^T, \end{aligned} \tag{18}$$

in which, $\mathbf{A}_i \in \mathbb{R}^{(s+1) \times 2s}$ and $\boldsymbol{\alpha}_i \in \mathbb{R}^{(s+1) \times 1}$ are defined as

$$\mathbf{A}_i = \begin{bmatrix} \mathbf{0}^T & \mathbb{1}^T \\ \mathbf{I} & \mathbf{I} \end{bmatrix}, \qquad \boldsymbol{\alpha}_i = \begin{bmatrix} \mathbf{0} \\ \mathbf{l_i} - \mathbf{p_i} \end{bmatrix}, \tag{19}$$

and $\mathbf{B}_i \in \mathbb{R}^{4s \times 2s}$ and $\boldsymbol{\beta}_i \in \mathbb{R}^{4s}$, are given by:

$$\mathbf{B}_i = \begin{bmatrix} \mathbf{0} & \mathbf{I} \\ \mathbf{0} & -\mathbf{I} \\ \mathbf{0} & \mathbf{T} \\ \mathbf{0} & -\mathbf{T} \end{bmatrix}, \quad \boldsymbol{\beta}_i = \begin{bmatrix} B_i^+ \\ B_i^- \\ \left(\frac{\mathbb{1}}{\Delta t} \right) \xi_i^0 \\ \left(\frac{\mathbb{1}}{\Delta t} \right) (C_i - \xi_i^0) \end{bmatrix}, \tag{20a}$$

where $\mathbf{0} \in \mathbb{R}^{s\times s}$ is a null matrix and $\mathbf{T} \in \mathbb{R}^{s\times s}_{\geq 0}$ a lower binary triangular matrix of all-1s with the elements such that

$$t_{uv} = \begin{cases} 1, & \forall u \geq v, \\ 0, & \text{otherwise}, \end{cases}$$

where u and v denote the row and column indices.

III. Distributed coordinated scheduling algorithms

A. Gradient-based algorithm

The first algorithm for solving the optimisation problem as shown in Problem (16) is based on Lagrangian duality where the objective function is augmented with a weighted sum of the constraints functions. Thus, the associated Lagrangian L to the optimisation Problem (16) becomes

$$L(\mathbf{x}, \boldsymbol{\lambda}, \boldsymbol{\mu}) = \frac{1}{2}\mathbf{x}^T\mathbf{Q}\mathbf{x} + \boldsymbol{\lambda}^T(\mathbf{A}\mathbf{x} - \boldsymbol{\alpha}) + \boldsymbol{\mu}^T(\mathbf{B}\mathbf{x} - \boldsymbol{\beta}), \quad (21)$$

where $\boldsymbol{\lambda}$ and $\boldsymbol{\mu}$ are the Lagrange multipliers. Based on Slaters Theorem, for a strictly feasible and convex primal problem sufficient conditions for strong duality hold and the solution to the Lagrange dual is a lower bound to the optimal value of the original problem. The equilibrium saddle point Karush-Kuhn-Tucker (KKT) conditions of the Lagrangian is defined as:

$$\nabla_x L = \mathbf{Q}\mathbf{x} + \mathbf{A}^T\boldsymbol{\lambda} + \mathbf{B}^T\boldsymbol{\mu} = \mathbf{0}, \quad (22a)$$

$$\nabla_\lambda L = \mathbf{A}\mathbf{x} - \boldsymbol{\alpha} = \mathbf{0}, \quad (22b)$$

$$\nabla_\mu L = \mathbf{B}\mathbf{x} - \boldsymbol{\beta} = \mathbf{0}, \quad (22c)$$

To converge to the saddle point, the primal and dual gradient method known as Arrow-Hurwicz-Uzawa (AHU) algorithm or as inexact Uzawa [1] is used which searches for the saddle-point of the Lagrangian by alternating steps in the direction of the gradients $-\nabla_{\mathbf{x}} L$, $\nabla_{\boldsymbol{\lambda}} L$ and $\nabla_{\boldsymbol{\mu}} L$.

The KKT conditions of (22) can be written in a distributed form as follows ($\forall i \in \{1, \ldots, m\}$).

$$\nabla_{x_i} L = \mathbf{Q}_i\mathbf{x}_i + \mathbf{f}_{ij} + \mathbf{A}_i^T\boldsymbol{\lambda}_i + \mathbf{B}_i^T\boldsymbol{\mu}_i = \mathbf{0}, \quad (23a)$$

$$\nabla_{\lambda_i} L = \mathbf{A}_i\mathbf{x}_i - \boldsymbol{\alpha}_i = \mathbf{0}, \quad (23b)$$

$$\nabla_{\mu_i} L = \mathbf{B}_i\mathbf{x}_i - \boldsymbol{\beta}_i = \mathbf{0}, \quad (23c)$$

where

$$\mathbf{Q}_i = \begin{bmatrix} \mathbf{I} & \mathbf{0} \\ \mathbf{0} & \rho\boldsymbol{\Gamma}_{\mathbf{ii}} \end{bmatrix}, \quad \mathbf{f}_{ij} = \begin{bmatrix} \mathbf{0} \\ \sum_{\substack{j=1 \\ j\neq i}}^{m} \boldsymbol{\rho}\boldsymbol{\Gamma}_{\mathbf{ij}}\mathbf{b}_j \end{bmatrix} \quad (24)$$

Therefore, a distributed gradient-based iterative algorithm to solve the problem (23) is given by

$$\mathbf{x}_i^{(k+1)} = \mathbf{x}_i^{(k)} - \tau\left[\mathbf{Q}_i\mathbf{x}_i^{(k)} + \mathbf{f}_{ij}^{(k)} + \mathbf{A}_i^T\boldsymbol{\lambda}_i^{(k)} + \mathbf{B}_i^T\boldsymbol{\mu}_i^{(k)}\right], \quad (25a)$$

$$\boldsymbol{\lambda}_i^{(k+1)} = \boldsymbol{\lambda}_i^{(k)} + \upsilon\left[\mathbf{A}_i\mathbf{x}_i^{(k)} - \boldsymbol{\alpha}_i\right], \quad (25b)$$

$$\boldsymbol{\mu}_i^{(k+1)} = \boldsymbol{\mu}_i^{(k)} + \upsilon\left[\mathbf{B}_i\mathbf{x}_i^{(k)} - \boldsymbol{\beta}_i\right]^+. \quad (25c)$$

where the scalar $\tau > 0$ and $\upsilon > 0$ are the primal and dual constant stepsizes and $[\cdot]^+$ denotes a projection on the positive orthant $\mathbb{R}^s_{\geq 0}$, such that $\mu_i^j = \max\{\mu_i^j, 0\}, \forall j \in \{1, \ldots, s\}$. Since the optimisation problem fulfils the condition of a convex quadratic-programming problem, selecting sufficiently small step sizes τ and υ will guarantee convergence of the algorithm [8].

As it can be seen from (25a), (25b) and (25c), except half of the equation (25a) associated with $\mathbf{b}_i$, all equations can be solved independently for each node. The dependent part is in $\mathbf{f}_{ij}$, which can be related to the average consensus algorithm [11] and depends on the grid topology. Equation (24) shows that to update $\mathbf{f}_{ij}^{(k)}$ we need $\mathbf{b}_j^{(k)}$ values from those nodes where $\boldsymbol{\Gamma}_{ij} \neq \mathbf{0}$. However, in a real large-scale distribution network, most of the $\boldsymbol{\Gamma}_{ij}$ are zero as there is a direct relationship between $\boldsymbol{\Gamma}$ and the Laplacian matrix $\mathbf{L}$ (equation (13)).

The equation (23) can be considered as the necessary conditions of m optimization sub-problems with coupled cost functions and decoupled constraints as follows:

$$\begin{aligned} &\min_{\mathbf{x}_i} \tfrac{1}{2}\mathbf{x}_i^T\mathbf{Q}_i\mathbf{x}_i + \mathbf{f}_{ij}^T\mathbf{x}_i \\ &\text{s.t.} \begin{cases} \mathbf{A}_i\mathbf{x}_i = \boldsymbol{\alpha}_i \\ \mathbf{B}_i\mathbf{x}_i \leq \boldsymbol{\beta}_i \end{cases} \end{aligned} \quad (26)$$

The gradient-based algorithm presented in (25) can be interpreted as a parallel solution of these sub-problems where each iteration is defined as one step in the sub-problems and the information exchange between them. In order to decrease the number of information exchange in the network, one can define the iteration as solving the sub-problems and then exchange the information. Regarding the sequence of solving the sub-problems, two different algorithm can be considered which will be explained in the next subsections [9].

B. Gauss-Seidel Algorithm

In order to solve the sub-problem (26), $\mathbf{f}_{ij}$ should be derived from the other sub-systems. By defining the cost function of i^{th} sub-problem as J_i, in each iteration of the Gauss-Seidel algorithm, more recent information from the other subsystems is considered:

$$\begin{aligned} &\bar{\mathbf{x}}_i^{(k+1)} = \arg\min_{\mathbf{x}_i} J_i\left(\mathbf{x}_1^{(k+1)}, \ldots, \mathbf{x}_{i-1}^{(k+1)}, \mathbf{x}_i^{(k)}, \ldots, \mathbf{x}_m^{(k)}\right), \\ &\mathbf{x}_i^{(k+1)} = \gamma_{GS}\,\bar{\mathbf{x}}_i^{(k+1)} + (1 - \gamma_{GS})\,\mathbf{x}_i^{(k)}, \end{aligned} \quad (27)$$

where γ_{GS} is the so-called relaxation parameter. It has been shown by [3], that if all sub-problems are quadratic programming problems (QP), the Gauss-Seidel algorithm is convergent for $0 < \gamma_{GS} < 2$. However, this parameter can be tuned for optimal convergence time. Since all sub-problems are in linear-quadratic format, they can be solved with very efficient QP algorithms. On the other hand, it was shown by [3], that when having the updated values of $\mathbf{x}_j$ from previous nodes (i.e. $\mathbf{x}_1^{(k+1)}$ to $\mathbf{x}_{i-1}^{(k+1)}$), the number of iterations will decrease, and hence the information exchange between nodes. However, the algorithm is not parallelizable and thus the utilization of the overall system per iteration is only $1/m$

percent of all nodes. The Gauss-Seidel algorithm solves the problem in a cascade fashion such that, qualitatively, the total processing time of the Gauss-Seidel algorithm is given by:

$$\tau_{pGS} = I_{GS} \left[\sum_{i=1}^{m} (\tau_{pi} + \tau_M) \right], \tag{28}$$

where I_{GS} is the number of iterations to converge, τ_{pi} is the processing time to solve the individual sub-problem at node i and τ_M is the one-way delay to transfer the estimate from node i to the other nodes.

C. Jacobi-based Algorithm

In order to make the latter distributed algorithm parallel implementable, equation (27) is modified as follows:

$$\begin{aligned} \bar{\mathbf{x}}_i^{(k+1)} &= arg\ \min_{\mathbf{x}_i} J_i \left(\mathbf{x}_1^{(k)}, \ldots, \mathbf{x}_{i-1}^{(k)}, \mathbf{x}_i^{(k)}, \mathbf{x}_{i+1}^{(k)}, \ldots, \mathbf{x}_m^{(k)} \right), \\ \mathbf{x}_i^{(k+1)} &= \gamma_J\, \bar{\mathbf{x}}_i^{(k+1)} + (1 - \gamma_J)\, \mathbf{x}_i^{(k)}, \end{aligned} \tag{29}$$

with $0 < \gamma_J \leq 1$. While higher values of γ_J can improve the convergence speed, the convergence is guaranteed for small values of γ_J.

In general, the Gauss-Seidel algorithm can converge much faster than Jacobi algorithm. However, when it comes to a large-scale networks with a large number of individual nodes, parallel processing of the sub-problems is important since, in contrast to (28), the overall processing time of the Jacobi algorithm is qualitatively given by

$$\tau_{pJ} = I_J \left\{ \max\left(\tau_{p1}, \tau_{p2}, \ldots, \tau_{pm}\right) + \tau_M \right\}, \tag{30}$$

where I_J is the number of iterations to converge, τ_{pi} is the processing time to solve the individual sub-problem at node i and τ_M is the one-way delay to transfer the estimate from node i to the other nodes.

IV. Case-Study Scenario

To illustrate the concept of the introduced coordinated battery scheduling in a VMG, we consider a scenario of 5 different residential buildings ($m = 5$), with individual load and production profiles. The scheduling time horizon is 1 day ($24h$) which is divided into 48 intervals ($s = 48$), such that $\Delta t = 0.5h$. Each building is equipped with photovoltaic installations (local source) as well as a co-located battery storage capacities. The batteries at the individual nodes have different capacities (C_i), between $3kWh$ and $10kWh$ and different maximum charge and discharge (B_i^+, B_i^-) limits. It is assumed that all buildings are connected to the same LV grid and that an overlaying communication topology, is given as shown in Figure 1.

The results obtained, by the introduced algorithms, for the given OP (16) are presented in Figure 3 and Figure 4, for $\rho = 0$ and $\rho = 10$, respectively.

Shown in these figures, is the optimal battery power flow b_i^j over the scheduling time horizon window T, as a stacked bar graph for each battery (in different grey-scales). A downward pointing bar means a battery is discharging in that period, whereas an upward point bar indicates that a battery charges. Further shown in Figure 3 and Figure 4, as a dashed line, is the original grid load profile, which is the sum over all loads minus productions, at the individual nodes. Note that if no storage capacities exist, such that $C_i = 0$ for all nodes, then this would be the resulting energy flow over the transformer substation as shown in Figure 1. If storage capacities are used, a residual grid profile remains which is indicated by the solid line.

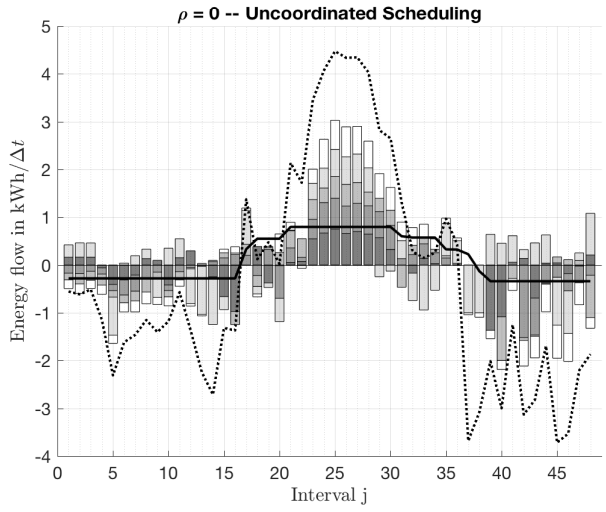

Fig. 3. Uncoordinated battery charge/discharge profile with $\rho = 0$, as stacked bar graphs, with $\sum_i^m (l_i^j - p_i^j)$ as dashed line and residual grid load $\sum_i \psi_i^j$ as solid line after dispatching, for each j. The colours of a bar indicate a battery at a node, and shows the charge discharge behaviour, b_i^j, for each interval j and node i, over the scheduling time horizon T.

The results obtained in these two simulation scenarios demonstrate a significant reduction in magnitude of the grid load prole, thus the feed-in peaks around noon as well as the peak loads in the morning and evening are smoothed, this is evident for both cases, $\rho = 0$ (uncoordinated) and $\rho = 10$ (coordinated). However, in contrast to the results obtained with coordination ($\rho = 10$), as shown in Figure 4, when no coordination takes place between the nodes ($\rho = 0$), as shown in Figure 3, mutual charging and discharging of storage capacities occurs. This can significantly be seen in Figure 3, in the range of intervals from $j = (0, \ldots, 20)$, and in $j = (31, \ldots, 48)$. Further, in Figure 4, it is evident that charge and discharge intervals between the different nodes are coordinated and no mutual charging /discharging occurs. Thus, in any period, all batteries are either charging or discharging.

V. Conclusions

A distributed method for coordinated scheduling of storage capacities, to be operated as a virtual was introduced. It is shown, that mutual charging and discharging of storage capacities can occur, if batteries are connected in the same grid and if the scheduling of individual storage devices is not coordinated. A formulation for coordination, as an objective function has been introduced, and a scheme how battery scheduling can be coordinated in order to operate them as a

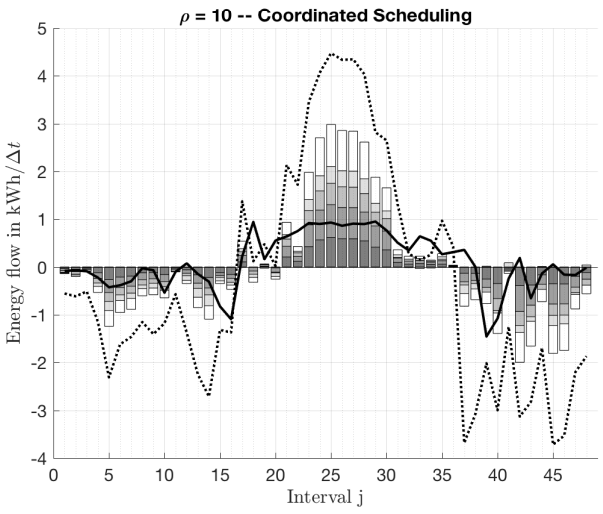

Fig. 4. Coordinated battery charge/discharge profile with $\rho = 10$, as stacked bar graphs, with $\sum_i^m (l_i^j - p_i^j)$ as dashed line and residual grid load $\sum_i \psi_i^j$ as solid line after dispatching, for each j. The colours of a bar indicate a battery at a node, and shows the charge discharge behaviour, b_i^j, for each interval j and node i, over the scheduling time horizon T..

virtual microgrid. It is shown that, by adding the coordination objective as a term to the local objective function, coordination between individual nodes can be incorporated. The Arrow-Hurwicz, the Gauss-Seidel and Jacobi algorithm have been qualified with respect to practical usefulness. Based on some qualitative analysis for the processing time of these distributed algorithms, it has been proposed that, when it comes to a large-scale networks, that a parallel processing algorithm outweighs a cascaded algorithm, which converge faster, i.e. in less number of iterations.

Based on two benchmark simulations, it is demonstrated that through the use of coordination, mutual charge/discharge of batteries is prevented. This is illustrated in a comparative study with a system where the scheduling does not take coordination between neighbouring nodes into account. The presented simulation scenarios highlight the advantage of coordination in a distributed EMS for scheduling of distributed batteries. Thus coordinated battery scheduling can significantly improve grid load by providing peak-shaving over a common transformer substation while simultaneously, mutual charge/discharging of batteries is prevented. Thus, the introduced cooperation scheme operates a system of distributed battery capacities more efficiently.

REFERENCES

[1] K.-J. Arrow, L. Hurwicz, H. Uzawa, H.-B. Chenery, S.-M. Johnson, S. Karlin, and T. Marschak. *Studies in linear and non-linear programming.* Stanford University Press, John Wiley & Sons, 1959.

[2] H. Asano, N. Hatziargyriou, R. Iravani, and C. Marnay. Microgrids: an overview of ongoing research, development, and demonstration projects. *IEEE Power Energy Magazine*, pages 78–94, 2007.

[3] D. P. Bertsekas and J. N. Tsitsiklis. *Parallel and distributed computation: numerical methods*, volume 23. Prentice hall Englewood Cliffs, NJ, 1989.

[4] R. Brehm, S. Mátéfi-Tempfli, and S. Top. Consensus based scheduling of storage capacities in a virtual microgrid. *Advances in Smart Systems Research (ISSN 2050-8662)*, 6(1):13–22, 2017.

[5] W. Hu, Z. Chen, and B. Bak-Jensen. Optimal operation strategy of battery energy storage system to real-time electricity price in denmark. In *IEEE PES General Meeting*, pages 1–7. IEEE, 2010.

[6] T. Huang and D. Liu. Residential energy system control and management using adaptive dynamic programming. In *Neural Networks (IJCNN), The 2011 International Joint Conference on*, pages 119–124. IEEE, 2011.

[7] I. Koutsopoulos, V. Hatzi, and L. Tassiulas. Optimal energy storage control policies for the smart power grid. In *Smart Grid Communications (SmartGridComm), 2011 IEEE International Conference on*, pages 475–480. IEEE, 2011.

[8] T. Mathew. *Domain decomposition methods for the numerical solution of partial differential equations*, volume 61. Springer Science & Business Media, 2008.

[9] I. Necoara, V. Nedelcu, and I. Dumitrache. Parallel and distributed optimization methods for estimation and control in networks. *Journal of Process Control*, 21(5):756–766, 2011.

[10] A. Nottrott, J. Kleissl, and B. Washom. Energy dispatch schedule optimization and cost benefit analysis for grid-connected, photovoltaic-battery storage systems. *Renewable Energy*, 55:230–240, 2013.

[11] R. Olfati-Saber, J. A. Fax, and R. M. Murray. Consensus and cooperation in networked multi-agent systems. *Proceedings of the IEEE*, 95(1):215–233, 2007.

[12] D. Olivares, A. Mehrizi-Sani, A. Etemadi, C. Canizares, R. Iravani, M. Kazerani, A. Hajimiragha, O. Gomis-Bellmunt, M. Saeedifard, R. Palma-Behnke, G. Jimenez-Estevez, and N. Hatziargyriou. Trends in microgrid control. *Smart Grid, IEEE Transactions on*, 5(4):1905–1919, July 2014.

[13] H. Quan, D. Srinivasan, and A. Khosravi. Integration of renewable generation uncertainties into stochastic unit commitment considering reserve and risk: A comparative study. *Energy*, 103:735–745, 2016.

[14] E. L. Ratnam, S. R. Weller, and C. M. Kellett. An optimization-based approach to scheduling residential battery storage with solar pv: Assessing customer benefit. *Renewable Energy*, 75:123–134, 2015.

[15] Y. Wang, X. Lin, M. Pedram, S. Park, and N. Chang. Optimal control of a grid-connected hybrid electrical energy storage system for homes. In *Design, Automation & Test in Europe Conference & Exhibition (DATE), 2013*, pages 881–886. IEEE, 2013.

[16] B. Zhao, M. Xue, X. Zhang, C. Wang, and J. Zhao. An mas based energy management system for a stand-alone microgrid at high altitude. *Applied Energy*, 143:251 – 261, 2015.